Controlling the fluorescence of ordinary oxazine dyes for single-molecule switching and superresolution microscopy

Jan Vogelsang, Thorben Cordes, Carsten Forthmann, Christian Steinhauer, and Philip Tinnefeld[1]

Angewandte Physik–Biophysik and Center for NanoScience, Ludwig-Maximilians-Universität, Amalienstrasse 54, 80799 Munich, Germany

Edited by Paul F. Barbara, University of Texas, Austin, TX, and approved April 10, 2009 (received for review November 21, 2008)

Fluorescent molecular switches have widespread potential for use as sensors, material applications in electro-optical data storages and displays, and superresolution fluorescence microscopy. We demonstrate that adjustment of fluorophore properties and environmental conditions allows the use of ordinary fluorescent dyes as efficient single-molecule switches that report sensitively on their local redox condition. Adding or removing reductant or oxidant, switches the fluorescence of oxazine dyes between stable fluorescent and nonfluorescent states. At low oxygen concentrations, the off-state that we ascribe to a radical anion is thermally stable with a lifetime in the minutes range. The molecular switches show a remarkable reliability with intriguing fatigue resistance at the single-molecule level: Depending on the switching rate, between 400 and 3,000 switching cycles are observed before irreversible photodestruction occurs. A detailed picture of the underlying photoinduced and redox reactions is elaborated. In the presence of both reductant and oxidant, continuous switching is manifested by ''blinking'' with independently controllable on- and off-state lifetimes in both deoxygenated and oxygenated environments. This ''continuous switching mode'' is advantageously used for imaging actin filament and actin filament bundles in fixed cells with subdiffraction-limited resolution.

electron transfer | molecular switch | sensor | single-molecule spectroscopy

Molecular switches are single-molecule devices, and hence they are key building-blocks for future, bottom-up nanotechnological devices in computers, data storages, (bio-) sensors, and displays. Furthermore, they are exciting molecules for triggered drug-release or for superresolution imaging (1–3). Molecular switches possess at least 2 stable states and can be converted between these states by external stimuli. These external stimuli can essentially be any kind of physical or chemical trigger, such as light, electricity, or certain chemical reactions. Fluorescence is a preferred transduction mechanism because of its ease of noninvasive detection with ultimate sensitivity (i.e., single-molecule sensitivity). For future devices and for superresolution microscopy, it is also important that the molecular switches can be operated at the level of single molecules. This requirement imposes further demands with respect to reliability, reproducibility, response time, and fatigue resistance. Although the single-molecule approach provides detailed information about the properties and mechanisms, only a few examples of fluorescent switches have been demonstrated (4, 5). Among the fluorescent switches, there are systems that use 2 different wavelengths for switching (photoswitchable molecules) (6–13), those that switch the efficiency of photoinduced electron transfer (14, 15) and those that respond to pH changes (15, 16).

Here, we show that based on a detailed understanding of their photophysics, ordinary, fluorescent dyes can act as single-molecule switches and sensors. By adapting the energy levels of the fluorescent dye to the redox conditions of the environment, we achieve exquisite control of the fluorescence properties of the dyes and the ability to switch the dyes on and off. This is achieved by using generic dark states, i.e., radical anion states, as reversible off-states that are stable in the absence of electron acceptors.

Commonly, unwanted and uncontrolled switching between bright "on" and dark "off" states is observed in single-molecule fluorescence transients and is referred to as "blinking." Besides photobleaching, dark states represent a main concern in many biomolecular single-molecule studies. Dark states often originate from stochastic transitions to the triplet state (17), or from radical ion states formed as a result of electron transfer reactions (18–21). Recently, an improved understanding of the underlying (redox) processes has led to ways to suppress photobleaching as well as triplet- and redox-blinking (22, 23). To gain control over blinking, we used oxazine dyes with low energy of the first reduced state and high energy of the first oxidized state, which stabilizes the reduced state and minimizes the influence of molecular oxygen that we cannot completely exclude in the experiments. We presumed that a reduced state could then be thermally stable. Switching is achieved for single immobilized DNA–oxazine constructs (oxazines: ATTO655, ATTO680, or ATTO700) in aqueous buffers through changing the redox environment from reducing for switching off to oxidizing for turning back on. We used single-molecule fluorescence spectroscopy (SMFS) and fluorescence correlation spectroscopy (FCS) to elucidate the photophysical pathways of these oxazine dyes and obtained a comprehensive model through correlation with thermodynamic data. Besides an intriguing switching performance, the dependence of the switching kinetics is used as a single-molecule redox-sensor (SMRS) for oxidants and reductants.

We demonstrate the potential of the molecular switch for far-field superresolution microscopy that is based on the subsequent localization of single molecules. Recently, the importance of dark states for far-field superresolution fluorescence microscopy using for example switchable molecules has been realized (2, 24, 25). The oxazine molecular switch offers some advantageous because the number of photons emitted during 1 on-time can be controlled, and the fluorescence control can be achieved in the presence of oxygen with impressive photostability. In this context, superresolution images of actin filaments immobilized on glass slides and actin bundles in fixed cells are presented.

Results and Discussion

Basics of Controlling Single-Molecule Fluorescence. To switch ordinary dye molecules we intended to use generic radical ion states as controllable off-states. Therefore, single oxazine dyes were attached to biotinylated double-stranded DNA that itself was immobilized on BSA/BSA-biotin-streptavidin coated cover slides according to published procedures (26). Measurements were carried out in aqueous buffers, which allowed enzymatic oxygen removal and

Author contributions: J.V. and P.T. designed research; J.V., T.C., C.F., and C.S. performed research; J.V., T.C., C.F., C.S., and P.T. analyzed data; and J.V., T.C., and P.T. wrote the paper.

The authors declare no conflict of interest.

This article is a PNAS Direct Submission.

[1]To whom correspondence should be addressed. E-mail: philip.tinnefeld@lmu.de.

This article contains supporting information online at www.pnas.org/cgi/content/full/0811875106/DCSupplemental.

addition of ascorbic acid (AA) as reductant and methylviologen (MV) as oxidant.

Although it is comparatively simple to prepare a fluorophore in its radical ion state through photoinduced electron transfer with a reductant or oxidant in solution (23, 25), it is challenging to stabilize the radical anion and prevent thermal return to the ground state. This requires careful removal of all electron acceptors from solution. By using enzymatic oxygen scavenging, the potential oxidant oxygen is removed to only low micromolar concentrations (27). We therefore selected oxazine derivatives with high reduction potential, i.e., the reduced state has very low energy so that reoxidation by oxygen with $E_{red} = -0.57$ V becomes inefficient (28). To describe the photophysical properties of single fluorophores taking into account the interaction with reducing and oxidizing agents, we used a 5-level scheme adapted to the thermodynamic parameters of the oxazine derivative ATTO655 (Fig. 1*A*). The energy levels were obtained by cyclic voltammetry as well as from steady-state absorption and fluorescence spectra [see supporting information (SI) *Text* for details): The zero–zero energy $E_{0,0} = 1.86$ eV, the first 1-electron reduction potential $E_{red} = -0.42$ V (vs. SCE), and the first 1-electron oxidation potential $E_{ox} = 1.31$ V (vs. SCE). The exact energy of the triplet state is not known, and it is assumed to be ≈0.3 eV lower than the singlet state (i.e., at ≈1.56 eV).

After placing a molecule in the laser focus, adding AA (100 μM) as reductant and removing oxygen, single-molecule fluorescence transients such as in Fig. 1*B* are obtained. A short fluorescent spike is observed terminated by rapid apparent photobleaching. In the presence of AA and MV (both 100 μM), however, single ATTO655 molecules show pronounced blinking with typical on- and off-times in the millisecond range (Fig. 1*C*). The fact that the fluorescence of ATTO655 resumes in the presence of the oxidant supports the idea that the fluorophore in Fig. 1*B* did not photobleach but instead entered a dark and—under these conditions stable—reduced state. The appearance of blinking for the investigated oxazines is attributed to inefficient recovery from the reduced state by MV although the presence of both reductant and oxidant have successfully removed blinking for some other fluorophores (23). Accordingly, the oxidant MV, which exhibits a reduction potential $E_{red} = -0.69$ V, is not able to efficiently depopulate the reduced state because of a calculated free energy for reoxidation of $\Delta G = 0.27$ eV. By using oxygen rather than MV, the off-times are considerably longer with $\tau_{off} = 1{,}800 \pm 1{,}000$ ms.

Switching Single Oxazine Molecules. To test the hypothesis that ATTO655 in the presence of only AA is not photobleached but indeed switched off to a stable reduced state, we scanned surfaces of immobilized dsDNA doubly labeled with Cy3B and ATTO655 using alternating laser excitation (Fig. 2) (29). Half of the time per pixel, the sample is excited with 533-nm light for excitation of the green dye Cy3B, and half of the time the red dye ATTO655 is excited by 640 nm. The first scan (Fig. 2*A*) was carried out in PBS containing ambient concentrations of oxygen, in which ATTO655 shows stable emission (see Fig. S1), to locate the doubly labeled DNAs. Molecules containing only Cy3B (Fig. 2, green), only ATTO655 (red), or both green and red dyes (yellow) were observed.

Before taking the second scan of the same area, oxygen was removed, and 100 μM AA was added. Under these conditions, the scanned area shows only green spots because ATTO655 rapidly enters a long-lived dark state (Fig. 2*B*). The green spots exhibit some dark pixels because of the transient formation of radical anions (23). Because the sample can slightly move upon buffer exchange, the green dye merely served to identify the same molecule positions as in the previous scan. After all red dyes are switched off, the buffer is exchanged again by washing the surface 3 times with PBS, which contains oxygen. In the subsequent scan (Fig. 2*C*), all ATTO655 molecules reappear. This procedure can be repeated several times and 3 such cycles with perfect switching of ATTO655 (see circled molecules) are shown in Fig. 2 *A*–*G*.

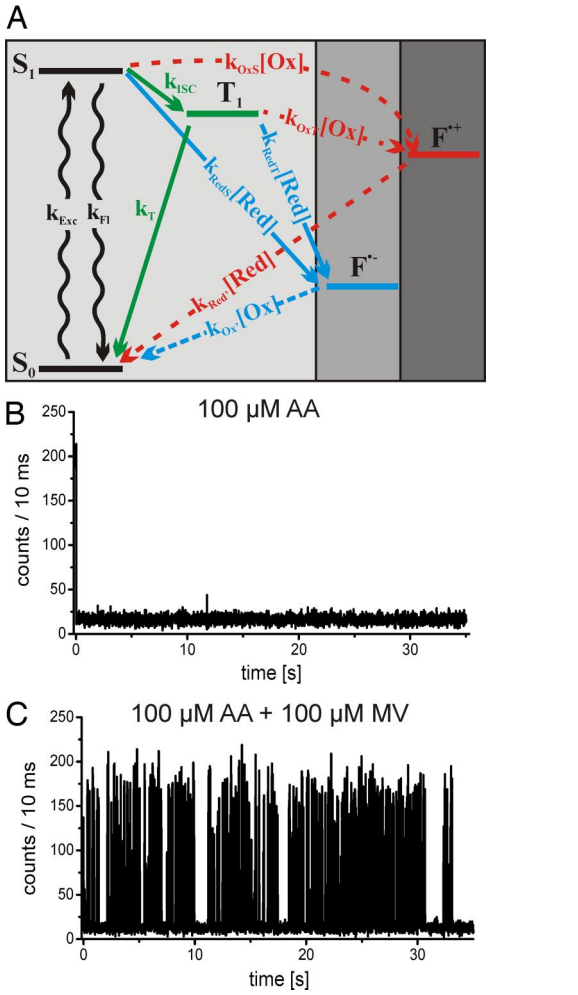

Fig. 1. Photoinduced processes of the fluorophore ATT0655. (*A*) Scheme. After excitation to the first excited singlet state S_1, fluorescence is emitted at rate k_{Fl} (neglecting nonradiative processes). Intersystem crossing competes with fluorescence and leads to the infrequent formation of triplet states T_1 with the rate constant k_{Isc}. The triplet state is depopulated by intersystem crossing with rate constant k_T or by electron transfer. This may occur either through oxidation by methylviologen (MV) forming a radical cation $F^{\bullet+}$ or through reduction by AA yielding a radical anion $F^{\bullet-}$. The radical ions could be recovered to singlet ground-state fluorophores by the complementary redox reaction. Direct electron transfer from the singlet manifold (k_{Reds}, k_{OxS}) has to be taken into account at higher redox-agent concentration. (*B* and *C*) Fluorescence transients of ATTO655-labeled dsDNA immobilized in aqueous environment after oxygen removal, addition of 100 μM AA (*B*) and additionally 100 μM MV (*C*), respectively. The transients are binned in 10 ms. Samples were excited at 640 nm with an average excitation intensity of 1.5 kW/cm^2.

Alternatively, MV can be used to switch ATTO655 on again, evidencing that it is the oxidation that turns ATTO655 back on. However, the efficient removal of MV from the chamber is more difficult and requires many more washing steps. The described switching procedure was also conducted with other oxazine dyes such as described in Fig. S2.

The data of Fig. 2 indicate that oxazines act as molecular switches where, in photodynamic equilibrium, the fluorescence is switched off under reducing conditions and switched on by using MV or oxygen. Important properties of molecular switches are (*i*) their bistability (i.e., the stability of the 2 states), (*ii*) the reliability and response time of switching, and (*iii*) their fatigue resistance (repeatability). Obviously, one critical issue is the stability of the reduced state. The observation of very long off-times of the reduced

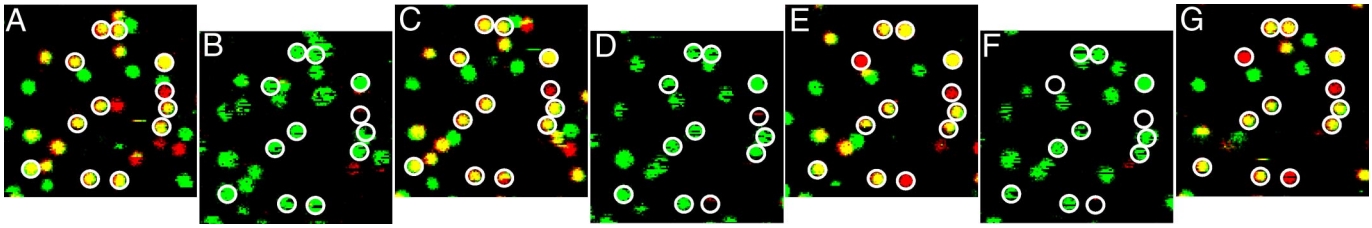

Fig. 2. Confocal fluorescence images (6 × 6 μm) of ATTO655-Cy3B-labeled dsDNA. The colors green and red encode for the overall fluorescence intensity after green and red excitation, respectively. dsDNA bearing the 2 dyes are hence visible as yellow spots. (*A*) The first image was acquired in PBS. (*B, D, F*) The second scan shows the same part of the cover slide after the buffer was deaerated and 100 μM AA was added. (*C, E, G*) Rinsing of the surface and refilling the chamber with standard PBS switches the molecules back into their fluorescent form. This cycle of reversible redox-switching of single ATTO655-molecules was repeated several times, 3 cycles are shown in *A–G*.

state in the absence of oxidants supports the idea that the radical-anion state is nonreactive and therefore is not considered a photobleaching pathway. To determine its thermal stability with respect to return to the ground state, single ATTO655 molecules were placed in the laser focus to record fluorescence transients in the presence of AA and after removal of oxygen, i.e., such as in Fig. 1*B*. After once being switched off, ≈50% of the molecules (50 investigated) remained in the off-state for the entire recording time of 120 s. The remaining ≈50% showed 1 or more small photon bursts on the time scale of minutes indicating transient recovery to the ground state. Because enzymatic oxygen scavenging reduces the oxygen concentration to ≈15 μM and does not completely deplete oxygen (27), the reduced state itself is likely thermally stable and requires a reaction partner such as oxygen to return to the ground state. The variability of thermal stability of the reduced state might then be related to the different accessibility of oxygen to the fluorophores because of local heterogeneity (9).

The repeatability of the switching procedure was tested in the presence and in the absence of oxygen. The buffer contained the reductant AA as well as the oxidant MV at concentrations of 100 μM, 250 μM, and 500 μM each. As shown in Fig. 1*C*, the molecules exhibited frequent blinking because of continuous switching. Fluorescence transients were recorded for ≈50 molecules until irreversible photodestruction occurred. During this period, the molecules went through 436 ± 32 up to 3,016 ± 669 switching cycles per molecule (see Fig. S3). This number of switching cycles is significantly higher than for other single-molecule switches (7–9, 11–13, 30). A decreasing concentration of oxidant and reductant resulted in a lower number of switching cycles (Fig. S3) because of a smaller cycling rate but comparable photobleaching probability. Measurements without oxygen removal showed an average increase in switching cycles of ≈60% because of the faster switching with the additional oxidant oxygen in the solution and, again, comparable photobleaching probability.

Quantification of Photoinduced Processes. The presence of reductant and oxidant at the same time offers the possibility of a "continuous switching mode," whose response time is influenced by the encounter rate with the redox agents (i.e., their concentrations) and the reaction rate constants. In the following, we studied the influence of different concentrations of the redox agents on the switching properties and elaborated the details of the photophysical scheme shown in Fig. 1*A*. First, we determined the intersystem crossing rate k_{isc} and the rate from the triplet state into the ground state k_T for ATTO655 in the presence of oxygen using FCS to $k_{isc} = (1.2 \pm 0.2) \times 10^5\ s^{-1}$ and $k_T = (6.6 \pm 2.2) \times 10^4\ s^{-1}$ (experimental results from FCS and further details are in *SI Text*, and see Fig. S4) (31). To determine the remaining rate constants, fluorescence transients of ATTO655 using different concentrations of AA and MV were recorded. Beginning with transients recorded at constant MV concentration (100 μM) and varying AA concentration, 2 components are observed in the autocorrelation of transients recorded at 10 μM AA (see Fig. S5*A* and details on data analysis in *SI Text*). We ascribe the long component to the formation of radical anions and the short component to the triplet state or the radical cation. Increasing the AA concentration, the short component vanishes, because triplets (and possibly oxidized states) are depopulated by AA more quickly and the on-times are reduced (Fig. 3 *A* and *D*). At the same time, the off-times remain constant (Fig. 3 *A* and *D*). When varying the concentration of MV and keeping the AA concentration constant at 100 μM, the on-times remain constant, and the off-times become shorter with increasing MV concentration (Fig. 3 *B* and *D*). If the formation of radical cations via k_{OxS} or k_{OxT} played a role, the on-times should become longer with increasing MV concentration. This is because the pathway through a radical cationic state would, at 100 μM AA, be very fast, i.e., without noticeable long off-state. Accordingly, the number of long off-states assigned to the reduced state should decrease with increasing MV concentration if the pathways through a reduced state and through an oxidized state competed. Thermodynamic considerations using the Rehm–Weller equation $\Delta G_{cs} = e[E_{ox} - E_{red}] - E_{0,0} + C$ (32), where e is the unit electrical charge and C the negligible Coulombic attraction energy, support the idea that oxidation from the triplet state ($\Delta G = 0.44$ eV, i.e., endergonic) and from the singlet state ($\Delta G = -0.14$ eV, i.e., slightly endergonic) cannot be detected because radical cation states of ATTO655 are not significantly populated, and the rates k_{OxS} and k_{OxT} are negligibly small. This part of the scheme is therefore shaded dark gray, and the corresponding red reaction arrows are dashed (Fig. 1*A*). Accordingly, all observed long dark states are reduced states that are depopulated by MV with rate $k_{Ox'}$[MV] and the short component in the autocorrelation of Fig. S5*A* can clearly be assigned to the triplet state with k_T in the absence of oxygen being $k_T = (5.5 \pm 2.5) \times 10^3\ s^{-1}$ (see *SI Text* for analysis). The independence of the action of AA and MV is a remarkable result because it implies that 2 variables are available to independently manipulate on- and off-state lifetimes over a broad range. AA controls the duration of the on-states, whereas MV influences the off-states. When both redox reagents are used simultaneously at equal concentrations, their effects are additive, further proving their independent applicability (Fig. 3 *C* and *F*). It is noteworthy that these dependencies hold in the absence (Fig. 3 *A–C*) and in the presence of oxygen (Fig. 3 *D–F*). Some changes in the absolute values are observed that are ascribed to the influence of oxygen on some of the rates such as k_T as well as on the effective AA activity.

Further experiments with terminally labeled ATTO655 showed that less reducing and oxidizing agents have to be used to obtain the same variations of on- and off-times compared with internally labeled ATTO655 DNA (see Fig. S6). This is explained by the better accessibility of the terminally labeled ATTO655 compared with the internally labeled ATTO655, which shows the tendency to be firmly bound to the DNA (see anisotropy and fluorescence lifetime measurements in *SI Text*). Similar results as for ATTO655 were

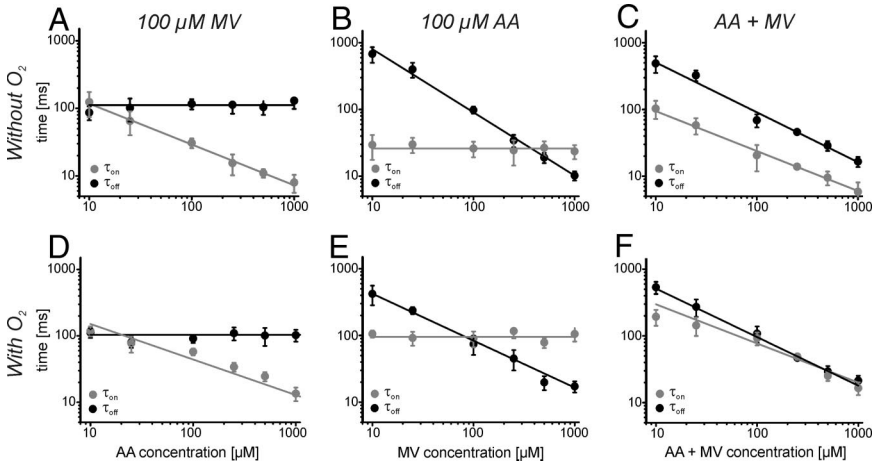

Fig. 3. Dependence of the on- and off-state lifetime τ_{on} and τ_{off} on the concentration of the reductant AA and the oxidant MV in the absence and presence of oxygen. (*A* and *D*) AA dependence of switching at constant 100 μM MV concentration. (*B* and *E*) MV dependence of switching at constant 100 μM AA concentration. (*C* and *F*) The on- and off-times with simultaneous change of MV and AA. The first row shows data measured without oxygen, whereas all data shown in the second row were measured in the presence of oxygen. The error bars indicate the standard deviation from the mean. The data were fitted by using an allometric function ($f(x) = a{\cdot}x^b$) to guide the eye.

obtained for the longer-wavelength oxazines ATTO680 and ATTO700 (see Figs. S2 and S7), emphasizing the general applicability.

After clarifying the independent role of AA and MV and the absence of oxidized states, we focused on the rate of reduction of the excited singlet state k_{RedS} and the rate for reduction of the excited triplet state k_{RedT} as well as the reoxidation rate $k_{Ox'}$, which are the remaining rates in Fig. 1*A*. Because of the long lifetime of the triplet state compared with the lifetime of the first excited singlet state, it is expected that k_{RedT} is responsible for the formation of radical anions at low reductant concentrations, whereas k_{RedS} becomes important in the millimolar range. The following discussion assumes that the number of photons, emitted during 1 on-time (on-counts N_{on}), is independent of excitation conditions. The on-counts can be described as the ratio of the sum of the rates depopulating the S_1 and T_1 states toward the ground state to the sum of rates that depopulate the S_1 and T_1 states yielding the radical anion:

$$N_{on}([AA]) = \frac{k_{Fl} + k_{Nr} + k_{Isc} \cdot \left(\frac{k_T}{k_T + k_{RedT} \cdot [AA]}\right)}{k_{RedS} \cdot [AA] + k_{Isc} \cdot \left(\frac{k_{RedT} \cdot [AA]}{k_T + k_{RedT} \cdot [AA]}\right)} \cdot \eta_{det} \cdot \phi_{fl}. \quad [1]$$

The term for N_{on} is additionally weighted with the detection efficiency η_{det} and the fluorescence quantum yield Φ_{fl}. With the fluorescence lifetime without additional quenching τ and the relation $\tau^{-1} = k_{Fl} + k_{nr} + k_{Isc}$, Eq.**1** can be rewritten as:

$$N_{on}([AA]) = \frac{\tau^{-1} + k_{Isc} \cdot \left(\frac{k_T}{k_T + k_{RedT} \cdot [AA]} - 1\right)}{k_{RedS} \cdot [AA] + k_{Isc} \cdot \left(\frac{k_{RedT} \cdot [AA]}{k_T + k_{RedT} \cdot [AA]}\right)} \cdot \eta_{det} \cdot \phi_{fl}. \quad [2]$$

Fig. 4 shows a plot of the on-counts N_{on} versus the AA concentration obtained from data such as in Fig. 3*A*.

The data could be well fitted by using Eq. **2** (Fig. 4, black line) with the ATTO655 fluorescence lifetime $\tau = 3.69$ ns, the intersystem crossing rate $k_{isc} = (1.2 \pm 0.2) \times 10^5\ s^{-1}$ and the triplet rate constant $k_T = (5.5 \pm 2.5) \times 10^3\ s^{-1}$, yielding rate constants of $k_{RedS} = (9.3 \pm 5.2) \times 10^7\ s^{-1}M^{-1}$, $k_{RedT} = (4.6 \pm 2.4) \times 10^7\ s^{-1}M^{-1}$ and the product $\eta_{det}{\cdot}\phi_{fl} = 0.08 \pm 0.03$. The faster rate constant from the singlet compared with the triplet is in accordance with expectations from Marcus theory because the driving force for the reaction is larger from the singlet state (33). Qualitatively, the S-shape of the graph can be understood by the reduction of the triplet state at low AA concentration that saturates at ≈500 μM AA. At higher AA concentrations, quenching of the singlet state becomes important and bends the graph downward again. The overall small values of the rate constants for the direct reduction of the singlet and triplet states is in good agreement with the fact that the addition of AA does not reduce the fluorescence lifetime up to 100 mM AA. By using reduced states formed from both singlet and triplet states enables an even broader dynamic range of dark state formation than shown in Fig. 3 with the possibility to generate dark states after, for example, 1 emitted photon, which is important for some superresolution microscopy approaches (34).

Finally, we determined the reoxidation rate $k_{Ox'}$ by MV from a fit to the τ_{off} graph in Fig. 3*B* to $k_{ox'} = (1.1 \pm 0.1) \times 10^5\ s^{-1}M^{-1}$ because $\tau_{off} = (k_{Ox'}{\cdot}[MV])^{-1}$. All rates determined are summarized in Table S1.

The presented results demonstrate an exquisite control of the oxazine fluorescence that even allows switching for a well-adapted

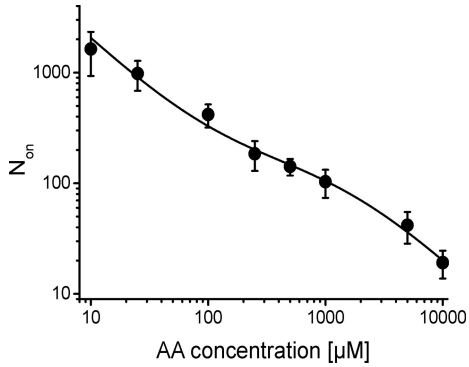

Fig. 4. Plot of the detected photons during an on-cycle, on-counts N_{on}, obtained from the fluorescence transients, versus the AA concentration. The error bars indicate the standard deviation from the mean. A fit using Eq. **2** is shown as black solid line.

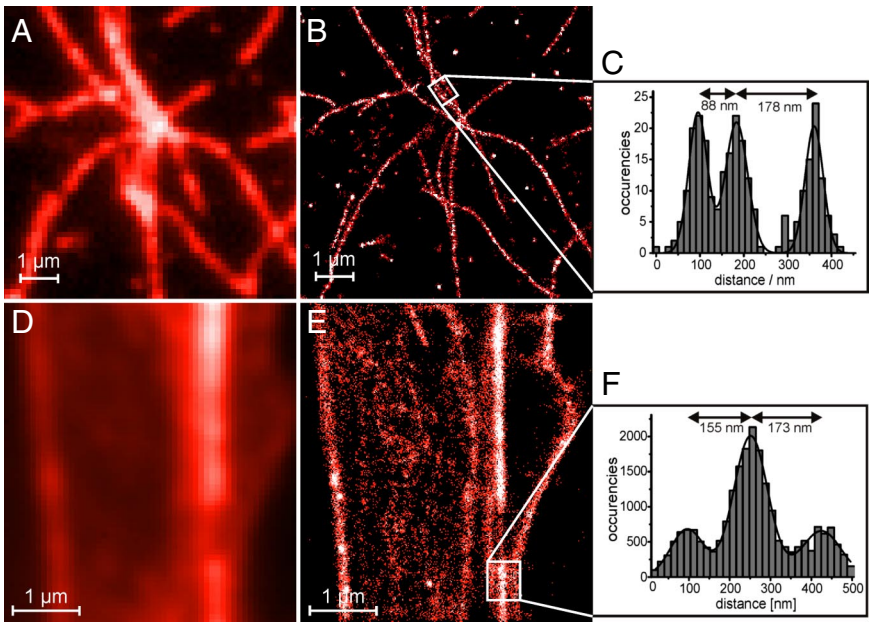

Fig. 5. Total internal reflection fluorescence microscopy of ATTO655-phalloidin-labeled single actin filaments (*A* and *B*) and bundled actin filaments in fixed NIH/3T3 cells (*D* and *E*). (*A* and *D*) TIRF microscopy images and (*B* and *E*) Blinkmicroscopy images with subdiffraction resolution. (*C* and *F*) Histograms over the regions marked with a white rectangle in *B* and *E* and the corresponding peak to peak distances derived from Gaussian fits. The images were recorded with reductant and oxidant concentrations optimized for imaging speed, fluorophore density, and excitation intensity (see *SI Text* for details).

fluorophore-environment system. This example shows that for construction of fluorescent switches, not only the molecule itself is important for the switching properties but that a fine balance with the experimental conditions can make molecules switchable that are not commonly considered switches. In principle, every fluorophore might possibly be switchable under the appropriate conditions. Vice versa, fluorophores might be constructed that show the required properties in a preset environment. Besides applications of such fluorophores as specific ion sensors or sensors of local redox conditions, e.g., inside living cells, the controllable fluorescence is of potential interests for superresolving fluorescence microscopy.

Superresolution Imaging with Single-Molecule Switches. Superresolution microscopy that circumvents the diffraction limit of light by subsequently localizing single photoswitchable molecules has opened up a field merging single-molecule fluorescence spectroscopy with diffraction-limit-breaking microscopy (2, 35–37). The common principle of subdiffraction resolution microscopy by subsequent single-molecule localizations is that only 1 fluorophore is active for a diffraction-limited area at any given time, and this fluorophore is localized by imaging with a sensitive camera. Thus, it is required that at any moment, most molecules are prepared in a dark state. Recently, it has been demonstrated that simply blinking of molecules, e.g., because of triplet formation, can be used, which drastically expands the range of usable fluorescent labels (24, 25, 38). Thus far, however, this blinking required oxygen removal (24, 25, 39), and the on-counts and off-times were poorly defined, although they determine the obtainable temporal and spatial resolution (25).

To demonstrate the potential of the presented molecular switch for superresolution microscopy, we recorded subdiffraction resolution "blink microscopy" images of ATTO655-phalloidin-stained actin filaments immobilized on cover slides (Fig. 5 *A* and *B*) and actin bundles in fixed cells (Fig. 5 *D* and *E*) (25). For data acquisition, 8,000–16,000 frames were recorded with total internal reflection fluorescence (TIRF) microscopy using appropriate concentrations of redox-active agents (see *SI Text* for details on superresolution imaging and analysis) (35, 36). The resolution of a blink microscopy image is mainly determined by the localization precision and the number of molecules that can be localized in a diffraction-limited spot (25). The on-counts N_{on} mainly determine the localization precision (40). Because reductants are used to control N_{on}, the localization precision is controlled simultaneously. This influence is exemplarily shown for the localization of single ATTO655-labeled dsDNA at 100 μM AA and 25 μM AA, yielding standard deviations of 26.8 and 18.7 nm, respectively (see Fig. S8). To increase the number of molecules localizable within a diffraction-limited area, the ratio of $\tau_{off}/(\tau_{off} + \tau_{on})$ should be as high as possible. Therefore, we reduced the on-times by using higher excitation intensities for imaging (16–50 kW/cm^2) compared with confocal measurements displayed in Fig. 3 and kept the off-times long by using low concentrations of oxidant. Thus, the adjustability of the on-counts and off-times allows choosing between spatial and temporal resolution. Fig. 5*A* shows a TIRF microscopy image of actin filaments immobilized on glass cover slides obtained from the first image frames when most molecules are still in their on-state. The reconstructed superresolution image in Fig. 5*B* clearly resolves structures that are not discernable in the standard TIRF image, as, for example, 3 actin fibers whose cross section profile is displayed in Fig. 5*C*. Using Gaussian fits, we determined the distance between 2 adjacent fibers to 88 nm (Fig. 5*C*). In cells, actin filaments form bundles that are observed in the TIRF image of NIH/3T3 fibroblasts labeled with ATTO655-phalloidin. These bundles are broader than the individual filaments shown in Fig. 5 *A* and *B*, but the blink microscopy image in Fig. 5*E* still resolves, for example, 3 actin bundles that are not resolved in the TIRF image (see Fig. 5 *D*–*F*).

The adjustability and the possibility to work in oxygenated environments are important advantages of the switchable oxazine fluorophores for superresolution microscopy. Additionally, these fluorophores are much more photostable in the presence of oxygen than, for example, rhodamine or cyanine derivatives, which is also likely related to their redox properties: Because of their high oxidation potential they are not efficiently oxidized by molecular oxygen, which is considered to be a key step in photobleaching pathways (41). Recalling that living cells themselves provide redox

active agents such as the reductants glutathione and ascorbic acid as well as oxidants such as quinone derivatives and oxygen, superresolution under in vivo conditions may become possible on the basis of the switchable molecules presented.

Conclusions

Recent advances in understanding fundamental processes governing the fluorescence of individual molecules are key to the success of many approaches in fluorescence sensors and superresolution microscopy. In this work, we demonstrate how fine adjustment of fluorophores and environmental conditions can be used to achieve exquisite control of the properties of single fluorophores and even to switch ordinary fluorophores on and off. Switching of single-oxazine dyes such as ATTO655, ATTO680, and ATTO700 was carried out with good stability of the dark state, fast response, unique reliability, and high photostability enabling ≈400–3,000 switching cycles with >260,000 detected photons. The generic nature of the dark state, i.e., the anionic state, indicates the universal character of the switching mechanism and suggests that for the development of switchable molecules, the interaction with the environment might be as important as the design of the molecular switch itself. By using oxidizing and reducing agents simultaneously, continuous switching was demonstrated and used for the elaboration of a detailed kinetic scheme. Importantly, the oxidant and the reductant represent 2 independent variables to control off- and on-times, respectively. This control of fluorescence was even carried out in the presence of oxygen and further used for superresolution blink microscopy of actin filaments immobilized on glass slides and actin bundles in fixed cells. Knowing the rules, it will only be a matter of time until fluorophores exhibiting adjusted redox blinking under the specific redox conditions of living cells will be demonstrated, further extending the toolbox of superresolution microscopies. The single-molecule-sensing capability can be used for localized redox sensing and has also been exploited to resolve the antiblinking mechanism of the vitamin E analogue Trolox as shown in refs. 22 and 42.

Materials and Methods

Details concerning fluorescent probes, e.g., sequences of DNA oligonucleotides and sample preparation are provided in *SI Text*.

Fluorescence transients of single dye conjugates and images were recorded by using a confocal scanning microscope equipped with 2 spectrally separated detectors. Excitation was carried out by a supercontinuum laser (SuperK Extreme; Koheras) in combination with acousto-optical tunable filters (AOTFnc-VIS; AA Optoelectronic). The spectral positions at 533 nm (spectral width of ≈2 nm, excitation of Cy3B) and 640 nm (spectral width of ≈2 nm, excitation of ATTO655) were chosen as excitation wavelengths. Average light intensities for acquisition of confocal fluorescence images were 1.5 kW/cm^2 at 533 nm and 4 kW/cm^2 at 640 nm. The laser beam was coupled into a single-mode fiber and subsequently into an oil-immersion objective (60×, N.A. 1.35, UPLSAPO 60XO; Olympus). The fluorescence was collected by using the same objective. The signal was spatially and spectrally filtered by using a 50-μm pinhole and a dichroic beam splitter (Dualband z533/633; AHF Analysentechnik), respectively. After spectrally splitting by a dichroic beam splitter (640DCXR; AHF Analysentechnik) and filtering (Brightline HC582/75, and ET-Bandpass 700/75, respectively; both AHF Analysentechnik), the fluorescence was detected by using 2 avalanche photodiodes (APD, SPCM-AQR-14; PerkinElmer). Further details about image scanning, measurement of intensity transients, and redox switching are provided in *SI Text*.

ACKNOWLEDGMENTS. We thank Hermann Gaub for stimulating discussions and Ann Fornof for proofreading the manuscript. This work was supported by the Biophotonics III Program of the BMBF/VDI (Grant 13N9234), the Nanosystems Initiative Munich and the Ludwig-Maximilians-Universität-Innovative ''Functional NanoSystems''. C.S. is grateful to the Elite Network of Bavaria (International Doctorate Program in NanoBioTechnology) for a doctoral fellowship.

1. Feringa BL (2001) *Molecular Switches* (Wiley-VCH, Weinheim, Germany), p 454.
2. Hell SW (2007) Far-field optical nanoscopy. *Science* 316:1153–1158.
3. Zhang X, Xiao Y, Qian X (2008) A ratiometric fluorescent probe based on FRET for imaging Hg^{2+} ions in living cells. *Angew Chem Int Ed* 47:8025–8029.
4. Holman MW, Liu R, Adams DM (2003) Single-molecule spectroscopy of interfacial electron transfer. *J Am Chem Soc* 125:12649–12654.
5. Cotlet M, et al. (2004) Probing conformational dynamics in single donor–acceptor synthetic molecules by means of photoinduced reversible electron transfer. *Proc Natl Acad Sci USA* 101:14343–14348.
6. Irie M (2000) Photochromism: Memories and switches-introduction. *Chem Rev* 100:1683.
7. Dickson RM, Cubitt AB, Tsien RY, Moerner WE (1997) On/off blinking and switching behavior of single molecules of green fluorescent protein. *Nature* 388:355–358.
8. Habuchi S, et al. (2005) Reversible single-molecule photoswitching in the GFP-like fluorescent protein Dronpa. *Proc Natl Acad Sci USA* 102:9511–9516.
9. Heilemann M, Margeat E, Kasper R, Sauer M, Tinnefeld P (2005) Carbocyanine dyes as efficient reversible single-molecule optical switch. *J Am Chem Soc* 127:3801–3806.
10. Bates M, Blosser TR, Zhuang X (2005) Short-range spectroscopic ruler based on a single-molecule optical switch. *Phys Rev Lett* 94:108101–108104.
11. Irie M, Fukaminato T, Sasaki T, Tamai N, Kawai T (2002) Organic chemistry: A digital fluorescent molecular photoswitch. *Nature* 420:759–760.
12. Fukaminato T, Sasaki T, Kawai T, Tamai N, Irie M (2004) Digital photoswitching of fluorescence based on the photochromism of diarylethene derivatives at a single-molecule level. *J Am Chem Soc* 126:14843–14849.
13. Fukaminato T, et al. (2007) Photochromism of diarylethene single molecules in polymer matrices. *J Am Chem Soc* 129:5932–5938.
14. Holman MW, et al. (2004) Studying and switching electron transfer: From the ensemble to the single molecule. *J Am Chem Soc* 126:16126–16133.
15. Zang L, Liu R, Holman MW, Nguyen KT, Adams DM (2002) A single-molecule probe based on intramolecular electron transfer. *J Am Chem Soc* 124:10640–10641.
16. Brasselet S, Moerner WE (2000) Fluorescence behavior of single-molecule pH-sensors. *Single Mol* 1:17–23.
17. Basche T, Kummer S, Brauchle C (1995) Direct spectroscopic observation of quantum jumps of a single- molecule. *Nature* 373:132–134.
18. Lu HP, Xie XS (1997) Single-molecule kinetics of interfacial electron transfer. *J Phys Chem B* 101:2753–2757.
19. Vosch T, et al. (2003) Probing Foerster type energy pathways in a first generation rigid dendrimer bearing two perylene imide chromophores. *J Phys Chem A* 107:6920–6931.
20. Kiel A, Kovacs J, Mokhir A, Kramer R, Herten DP (2007) Direct monitoring of formation and dissociation of individual metal complexes by single-molecule fluorescence spectroscopy. *Angew Chem Int Ed* 46:5049–5052.
21. Zondervan R, Kulzer F, Orlinskii SB, Orrit M (2003) Photoblinking of rhodamine 6G in poly(vinyl alcohol): Radical dark state formed through the triplet. *J Phys Chem A* 107:6770–6776.
22. Rasnik I, McKinney SA, Ha T (2006) Nonblinking and long-lasting single-molecule fluorescence imaging. *Nat Methods* 3:891–893.
23. Vogelsang J, et al. (2008) A reducing and oxidizing system minimizes photobleaching and blinking of fluorescent dyes. *Angew Chem Int Ed* 47:5465–5469.
24. Folling J, et al. (2008) Fluorescence nanoscopy by ground-state depletion and single-molecule return. *Nat Methods* 5:943–945.
25. Steinhauer C, Forthmann C, Vogelsang J, Tinnefeld P (2008) Superresolution microscopy on the basis of engineered dark states. *J Am Chem Soc* 130:16840–16841.
26. Okumus B, Wilson TJ, Lilley DMJ, Ha T (2004) Vesicle encapsulation studies reveal that single molecule ribozyme heterogeneities are intrinsic. *Biophys J* 87:2798–2806.
27. Aitken CE, Marshall RA, Puglisi JD (2008) An oxygen scavenging system for improvement of dye stability in single-molecule fluorescence experiments. *Biophys J* 94:1826–1835.
28. Holleman AF, Wiberg E (1995) *Lehrbuch der Anorganischen Chemie* (de Gruyter, New York).
29. Kapanidis AN, et al. (2005) Alternating-laser excitation of single molecules. *Acc Chem Res* 38:523–533.
30. Andresen M, et al. (2007) Structural basis for reversible photoswitching in Dronpa. *Proc Natl Acad Sci USA* 104:13005–13009.
31. Widengren J, Rigler R (1996) Mechanisms of photobleaching investigated by fluorescence correlation spectroscopy. *BioImaging* 4:149–157.
32. Rehm D, Weller A (1970) Kinetics of fluorescence quenching by electron and hydrogen-atom transfer. *Isr J Chem* 8:259–271.
33. Marcus RA (1956) On the theory of oxidation–reduction reactions involving electron transfer. *J Chem Phys* 24:966–978.
34. Enderlein J (2005) Breaking the diffraction limit with dynamic saturation optical microscopy. *Appl Phys Lett* 87:094105/094101–094105/094103.
35. Betzig E, et al. (2006) Imaging intracellular fluorescent proteins at nanometer resolution. *Science* 313:1642–1645.
36. Rust MJ, Bates M, Zhuang X (2006) Sub-diffraction-limit imaging by stochastic optical reconstruction microscopy (STORM). *Nat Methods* 3:793–795.
37. Hess ST, Girirajan TP, Mason MD (2006) Ultra-high resolution imaging by fluorescence photoactivation localization microscopy. *Biophys J* 91:4258–4272.
38. van de Linde S, Kapser R, Heilemann M, Sauer M (2008) Photoswitching microscopy with standard fluorophores. *Appl Phys B* 93:725–731.
39. Bock H, et al. (2007) Two-color far-field fluorescence nanoscopy based on photoswitchable emitters. *Appl Phys B* 88:161–165.
40. Thompson RE, Larson DR, Webb WW (2002) Precise nanometer localization analysis for individual fluorescent probes. *Biophys J* 82:2775–2783.
41. Hinkeldey B, Schmitt A, Jung G (2008) Comparative photostability studies of BODIPY and fluorescein dyes by using fluorescence correlation spectroscopy. *ChemPhysChem* 9:2019–2027.
42. Cordes T, Vogelsang J, Tinnefeld P (2009) On the mechanism of trolox as antiblinking and antibleaching reagent. *J Am Chem Soc* 131:5018–5019.